

# Understanding Li Diffusion in Li-Intercalation Compounds

ANTON VAN DER VEN,<sup>\*,†</sup> JISHNU BHATTACHARYA,<sup>‡</sup> AND ANNA A. BELAK<sup>†</sup>

<sup>†</sup>*Department of Materials Science and Engineering, The University of Michigan, 2300 Hayward Street, Ann Arbor, Michigan 48109, United States, and*

<sup>‡</sup>*Department of Materials Science and Engineering, Northwestern University, 2220 Campus Drive, 2036, Evanston, Illinois 60208, United States*

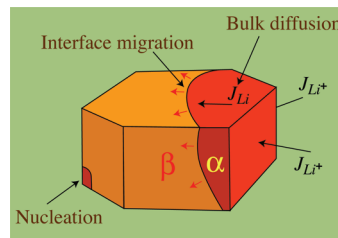
RECEIVED ON DECEMBER 13, 2011

## CONSPECTUS

Intercalation compounds, used as electrodes in Li-ion batteries, are a fascinating class of materials that exhibit a wide variety of electronic, crystallographic, thermodynamic, and kinetic properties. With open structures that allow for the easy insertion and removal of Li ions, the properties of these materials strongly depend on the interplay of the host chemistry and crystal structure, the Li concentration, and electrode particle morphology. The large variations in Li concentration within electrodes during each charge and discharge cycle of a Li battery are often accompanied by phase transformations. These transformations include order–disorder transitions, two-phase reactions that require the passage of an interface through the electrode particles, and structural phase transitions, in which the host undergoes a crystallographic change. Although the chemistry of an electrode material determines the voltage range in which it is electrochemically active, the crystal structure of the compound often plays a crucial role in determining the shape of the voltage profile as a function of Li concentration.

While the relationship between the voltage profile and crystal structure of transition metal oxide and sulfide intercalation compounds is well characterized, far less is known about the kinetic behavior of these materials. For example, because these processes are especially difficult to isolate experimentally, solid-state Li diffusion, phase transformation mechanisms, and interface reactions remain poorly understood. In this respect, first-principles statistical mechanical approaches can elucidate the effect of chemistry and crystal structure on kinetic properties.

In this Account, we review the key factors that govern Li diffusion in intercalation compounds and illustrate how the complexity of Li diffusion mechanisms correlates with the crystal structure of the compound. A variety of important diffusion mechanisms and associated migration barriers are sensitive to the overall Li concentration, resulting in diffusion coefficients that can vary by several orders of magnitude with changes in the lithium content. Vacancy clusters, groupings of vacancies within the crystal lattice, provide a common mechanism that mediates Li diffusion in important intercalation compounds. This mechanism emerges from specific crystallographic features of the host and results in a strong decrease of the Li diffusion coefficient as Li is added to an already Li rich host. Other crystallographic and electronic factors, such as the proximity of transition metal ions to activated states of hops and the occurrence of electronically induced distortions, can result in a strong dependence of the Li mobility on the overall Li concentration. The insights obtained from fundamental studies of ionic diffusion in electrode materials will be instrumental for physical chemists, chemical engineers, synthetic chemists, and materials and device designers who are developing these technologies.



## Introduction

A Li-ion battery is unique among devices in how it relies on its material components during use. In a lithium battery, the electrode materials undergo dramatic changes in Li concentration during each charge and discharge cycle. Large changes of composition in the solid state are often

accompanied by phase changes. In fact, the kinetic processes that occur in the electrodes of a Li battery during each charge and discharge cycle are not unlike the complex phase transformations that are often exploited during high temperature processing of materials, involving long-range atomic transport and crystallographic changes.

The difference with materials synthesis, which is a one-time event, is that the dramatic structural and chemical changes that transpire in Li battery electrodes occur every time the battery is charged and discharged and in large part determine battery performance and lifetime.

The Li-battery designs in current use typically consist of a carbon (graphite) based anode and a transition metal oxide intercalation host as cathode. In the charged state, Li ions reside between the graphitic sheets in the anode while the transition metal oxide is Li deficient. Thermodynamically, the Li ions between the graphitic layers would much rather occupy the empty interstitial sites of the transition metal oxide cathode material. However, a spontaneous chemical reaction involving the transfer of Li from the anode to the cathode is prevented in a Li battery due to the presence of the electrolyte, which only allows passage of  $\text{Li}^+$  ions (as opposed to neutral Li atoms). The  $\text{Li}^+$  can only trickle through the electrolyte if an external circuit through which electrons can travel connects the anode and the cathode. In this way, the resulting electrochemical device converts the change in free energy due to the transfer of Li from the anode to the cathode into electrical work.

Changes in Li composition affect the electronic properties and phase stability of the active electrode materials. The ability to shuttle Li back and forth between anode and cathode relies to a large extent on the kinetics of Li diffusion and the nature and rates of phase transformations within the electrode materials (Figure 1). While several intercalation compounds exhibit solid solution behavior over the entire composition domain, most undergo a variety of first-order phase transformations as the Li composition changes. Often phase transformations in intercalation compounds are between crystallographically very similar phases. Li extraction from  $\text{LiFePO}_4$ , for example, occurs through a first order phase transformation to an  $\text{FePO}_4$  host structure having the same crystal structure as  $\text{LiFePO}_4$ . Li insertion into graphite, in contrast, results in a change of the graphene stacking sequence from ABAB to AA stacking. Similar stacking sequence changes occur in layered cathode materials such as  $\text{Li}_x\text{CoO}_2$ .<sup>1–3</sup>

While the kinetics that emerge upon Li removal and reinsertion into intercalation compounds can be complex and varied, a common kinetic phenomenon of all intercalation compounds is the solid-state diffusion of Li from the electrode–electrolyte interface to the interior of the electrode particles (Figure 1). Since the Li concentration can vary from dilute to fully concentrated limits, diffusion in intercalation compounds occurs at nondilute concentrations where

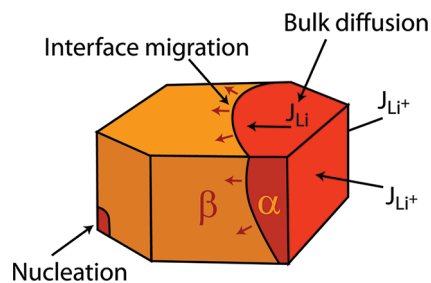


**FIGURE 1.** A variety of kinetic phenomena, including Li diffusion and first-order phase transformations involving nucleation and interface migration, occur within individual electrode particles during each charge and discharge cycle of a Li-ion battery.

interactions among different Li ions are important. Furthermore, intercalation compounds for Li-batteries exhibit a wide variety of crystal structures that offer a range of interstitial sites having one-, two-, and three-dimensional connectivities.

Accurate experimental measurements of Li diffusion coefficients have proven challenging, as most are indirectly derived from the dynamic response of an entire electrochemical cell for which geometry and competing kinetic processes are poorly characterized. Powerful local probes such as NMR have provided important insight about atomic hop mechanisms,<sup>4–7</sup> but have so far shed little light on collective Li transport and the resultant macroscopic diffusion coefficient appearing in Fick's law. This has prevented the establishment of a clear understanding of the role of chemistry and crystal structure on Li diffusion and its concentration dependence, which is of crucial importance in improving charge and discharge capabilities. A variety of first-principles statistical mechanical studies have been successful at elucidating collective transport mechanisms and their dependence on intercalation compound chemistry and crystal structure.<sup>8–14</sup> Here we review key insights gained from these studies. We start with a brief overview of fundamental crystallographic and thermodynamic properties of intercalation electrode materials followed by a more in depth description of diffusion mechanisms and their relationship to macroscopic metrics of Li transport.

## Crystallography

Many of the important transition metal oxide and sulfide intercalation compounds consist of a close-packed oxygen or sulfur sublattice, which provides an array of octahedral and tetrahedral interstitial sites that can be occupied by the transition metal and Li cations (Figure 2).<sup>15,16</sup> The oxygen sublattice of layered transition metal oxides

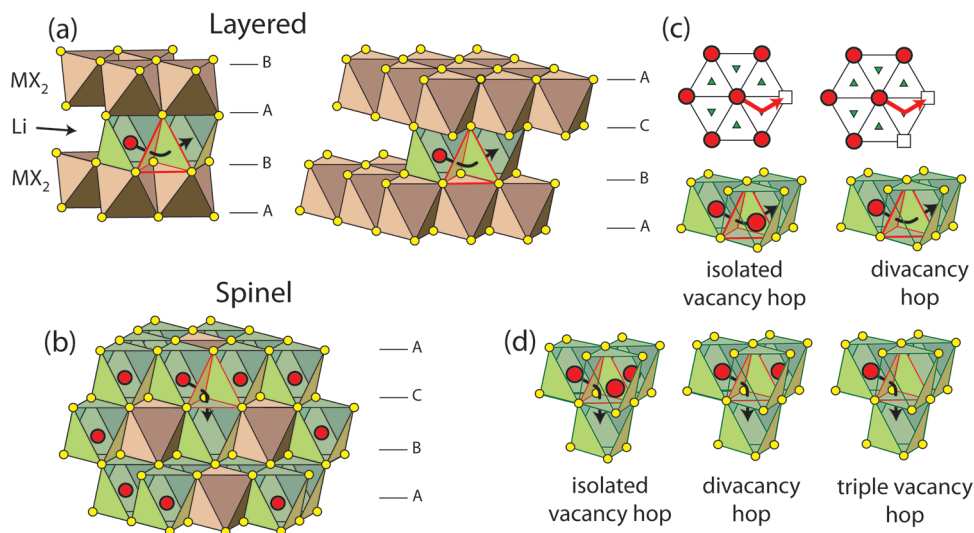


**FIGURE 2.** Important crystal structures and Li hop mechanisms in common intercalation compounds. Many intercalation compound chemistries have either (a) a layered crystal structure (with an ABAB or ABC stacking of a close-packed anion sublattice) or (b) a spinel crystal structure characterized by a three-dimensional interstitial network for Li ions. Diffusion in these crystal structures is often mediated by vacancy clusters (divacancies in the layered form and triple and divacancies in the spinel form) if Li occupies octahedral sites.

(e.g., Li<sub>x</sub>CoO<sub>2</sub>, Li<sub>x</sub>(Co<sub>0.33</sub>Ni<sub>0.33</sub>Mn<sub>0.33</sub>)O<sub>2</sub>) and of spinel transition metal oxides have an ABCABC stacking sequence. Meanwhile the anion sublattice of layered LiTiS<sub>2</sub> and delithiated CoO<sub>2</sub> have an ABAB stacking sequence. In most of these compounds, Li prefers to occupy octahedral interstitial sites. Spinel Li<sub>x</sub>M<sub>2</sub>O<sub>4</sub> (M=Mn or Ti) is an exception with Li preferring tetrahedral sites when *x* is less than 1. Crystal structures such as anatase TiO<sub>2</sub> can also be described as having an ABCABC stacking of close-packed oxygen planes with Ti ordered over half the octahedral sites. The particular Ti ordering breaks the symmetry of the cubic ABCABC stacking generating a lattice with tetragonal symmetry. Even more complex chemistries such as Li<sub>x</sub>FePO<sub>4</sub> in the olivine structure can be viewed as having an ABAB oxygen sublattice with Li, Fe, and P occupying a subset of octahedral and tetrahedral interstitial sites.

## Thermodynamics

While abstract thermodynamic quantities such as free energies and chemical potentials are often only obtainable through indirect measurement, simply tracking the voltage of a Li battery provides direct access to the Li chemical potential within the electrodes. According to the Nernst equation, the voltage (EMF) measured across the anode and cathode is equal to the difference of the Li chemical potentials between the electrodes according to

$$\Phi = \frac{(\mu_{\text{Li}}^{\text{cathode}} - \mu_{\text{Li}}^{\text{anode}})}{e}$$

where *e* is the charge of an electron and the chemical potentials  $\mu_{\text{Li}}^{\text{anode}}$  and  $\mu_{\text{Li}}^{\text{cathode}}$  are expressed in eV per Li atom. The voltage curve of an electrode material when measured with respect to a Li metal reference electrode (for which the Li chemical potential,  $\mu_{\text{Li}}^{\text{anode}}$ , remains constant during charge and discharge) is therefore linearly related to minus the Li chemical potential within the electrode. The chemical potential of interstitial Li in an intercalation compound in turn is equal to the derivative of the free energy of the material with respect to Li concentration according to

$$\mu_{\text{Li}} = \frac{\partial g}{\partial x}$$

Here *g* is the Gibbs free energy per Li<sub>x</sub>MA formula unit, where MA represents the host chemistry (e.g., CoO<sub>2</sub>, FePO<sub>4</sub>, or Mn<sub>2</sub>O<sub>4</sub> with M being the transition metal and A the anion unit) and *x* denotes the fraction of available interstitial sites occupied by Li. Graphically, the Li chemical potential within an intercalation compound at a particular composition *x* is equal to the slope of the free energy *g* at that composition as illustrated in Figure 3. A voltage measurement, therefore, provides direct information about the thermodynamic properties of electrode materials, including the Li chemical potential, the Gibbs free energy and derived properties such as entropy. Any changes in crystal structure or chemistry of the electrode

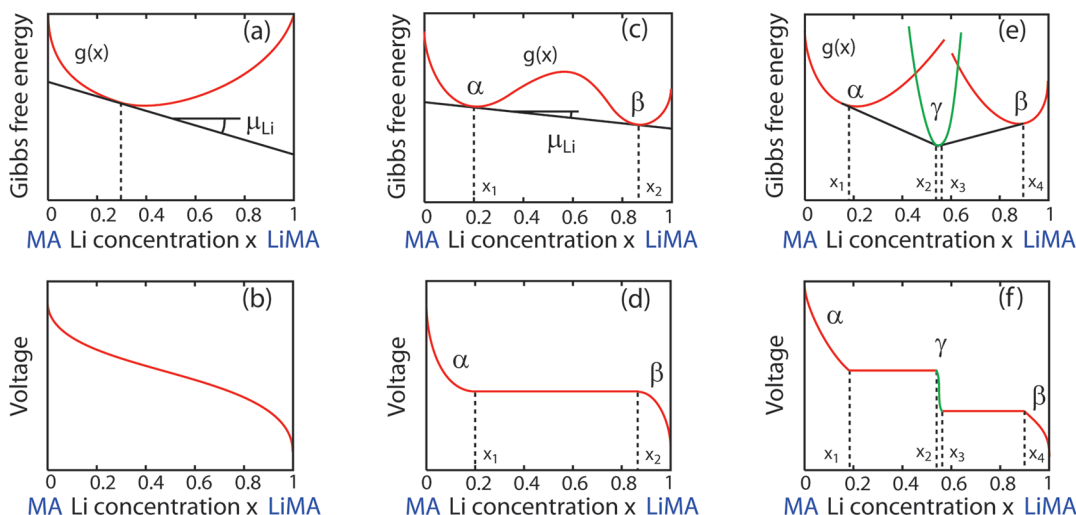


**FIGURE 3.** Voltage curves are linearly related to the slope of the free energy of the electrode material. See the text for a description of the various types of voltage curves and their relation to phase transformations.

material will affect its Gibbs free energy and Li-chemical potential and hence the voltage.

The straightforward connection between a measurable voltage curve and the Gibbs free energy means that the occurrence and nature of phase transformations due to variations in Li concentration will have clear signatures in the voltage profile. This is illustrated in Figure 3. If the electrode host material forms a solid solution with Li (Figure 3a) as occurs in  $\text{Li}_x\text{TiS}_2$ , it will exhibit a smooth sloping voltage curve as illustrated in Figure 3b. If, however, Li insertion is accompanied by a first-order phase transformation from a Li poor phase,  $\alpha$ , to a Li rich phase,  $\beta$ , as occurs in  $\text{Li}_x\text{FePO}_4$ , it will have a free energy curve as illustrated in Figure 3c, exhibiting two local minima (assuming the host maintains the same crystal structure). The Li chemical potential inside the miscibility gap (between  $x_1$  and  $x_2$  in Figure 3c) is constant as the free energy of the two-phase mixture resides on the common tangent to the free energy wells corresponding to  $\alpha$  and  $\beta$ . This results in a plateau in the voltage curve as illustrated in Figure 3d. Steps in the voltage profile appear if an intermediate phase is stable (Figure 3c and f). Often intermediate phases emerge at stoichiometric compositions where the Li ions and vacancies order in an energetically favorable arrangement over the interstitial sites of the host or where an energetically favorable interstitial site becomes fully filled as occurs in spinel  $\text{LiMn}_2\text{O}_4$ .

It is customary in thermochemistry to compare the actual thermodynamic properties of a particular material to that of a thermodynamically ideal solution. *Thermodynamic ideality* in the present context refers to hypothetical intercalation

compounds in which interactions between Li ions over the interstitial sites of the host can be neglected. The energy of the intercalation compound then depends linearly on Li concentration and is independent of how Li ions and vacancies at fixed Li concentration arrange themselves. The free energy per interstitial site of an intercalation compound  $\text{Li}_x\text{MA}$  is then (for systems with one type of Li interstitial site)

$$g(x) = g_0 + \varepsilon x + kT [x \ln x + (1 - x) \ln(1 - x)]$$

where  $g_0$  is the free energy of the host MA in the absence of Li and  $\varepsilon$  is the free energy change minus the configurational entropy per Li added to the host. The third term accounts for the ideal solution configurational entropy arising from the many possible ways of distributing Li ions and vacancies over the interstitial sites of the host. The voltage, linearly related to minus the Li chemical potential, of an ideal solution cathode relative to a metallic Li reference anode is then equal to

$$\Phi = \frac{\left[ \varepsilon + kT \ln \left( \frac{x}{1-x} \right) - \mu_{\text{Li}}^0 \right]}{e}$$

where  $\mu_{\text{Li}}^0$  is the free energy per atom of metallic Li and is a constant. It has a shallow sloping variation with Li concentration similar to that illustrated in Figure 3b.

The voltage profiles of most intercalation compounds deviate strongly from thermodynamic ideality. Furthermore, the crystal structure of the intercalation compound often has a significant influence on the shape of the voltage curve. The voltage profiles of spinel intercalation compounds, such as  $\text{Li}_x\text{Mn}_2\text{O}_4$  and  $\text{Li}_{1+x}\text{Ti}_2\text{O}_4$ , for example, are quite distinct

from those of layered or olivine intercalation compounds. Layered intercalation compounds such as  $\text{Li}_x\text{CoO}_2$  and  $\text{Li}_x(\text{Co}_{1/3}\text{Ni}_{1/3}\text{Mn}_{1/3})\text{O}_2$  have relatively flat, though sloping voltage profiles. Spinel intercalation compounds, in contrast, typically exhibit a large voltage step at half capacity (i.e., at  $x = 1$  in  $\text{Li}_x\text{Mn}_2\text{O}_4$ ), while the voltage profile of olivine  $\text{Li}_x\text{FePO}_4$  is a simple plateau between  $x = 0$  and  $x = 1$ .<sup>16</sup>

First-principles statistical mechanical approaches accounting for configurational degrees of freedom can predict the shape of the voltage curves of intercalation compounds with remarkable accuracy. These approaches rely on a cluster expansion formalism that in combination with ab initio electronic structure methods and Monte Carlo simulations enable a prediction of finite temperature phase stability and voltage curves. Examples of systems studied in this manner include  $\text{Li}_2\text{CoO}_2$ ,<sup>17,18</sup>  $\text{LiFePO}_4$ ,<sup>19</sup>  $\text{Li}_x(\text{Ni}_{0.5}\text{Mn}_{0.5})\text{O}_2$ ,<sup>20</sup>  $\text{LiTiO}_2$ ,<sup>12</sup>  $\text{LiTiS}_2$ ,<sup>11,14</sup> and  $\text{Li}_x\text{C}_6$ .<sup>13</sup>

## Kinetics: Li Transport

While the shape of the voltage profile and the intrinsic storage capacity are determined by thermodynamic properties of the intercalation compound, the rate with which a Li battery can be charged and discharged depends on kinetic properties such as the Li mobility and phase transformation mechanisms. A convenient starting point to describe Li diffusion within an intercalation compound is at the macroscopic phenomenological level where a net flux of Li ions can be related to a gradient in Li chemical potential according to

$$J_{\text{Li}} = -L\nabla\mu_{\text{Li}}$$

The kinetic coefficient  $L$  is a materials property that depends on the chemistry and crystal structure of the intercalation compound as well as the local Li concentration within the host. Since electrode materials must have some degree of electronic conductivity, often significantly larger than Li mobilities, it is usually justified to neglect electric fields and their effect on Li transport. Possible exceptions include  $\text{Li}_x\text{FePO}_4$  where evidence for polaronic electron transport suggests that Li and electron transport may need to be treated on an equal footing<sup>21,22</sup> or intercalation compounds that are semiconducting as, for example,  $\text{Li}_x\text{CoO}_2$  when  $x$  is greater than 0.95. Proceeding under the assumption of high electron mobilities, we can relate the kinetic coefficient  $L$  to a Li mobility  $M$  according to  $L = xM/\Omega$  with  $\Omega$  being the volume of the crystal per Li site (an ionic mobility

relates a Li velocity in the crystal to a gradient in chemical potential, i.e.  $\vec{v} = -M\nabla\mu$ ). The mobility,  $M$ , is itself an implicit function of the Li concentration, but does not directly scale with  $x$ , converging instead to a constant value as  $x$  goes to zero. The phenomenological flux expression can be converted into a Fickian flux expression by simple application of the chain rule of differentiation, yielding

$$J_{\text{Li}} = -D\nabla C_{\text{Li}}$$

where  $D$  is the chemical diffusion coefficient and  $C_{\text{Li}}$  is the local Li concentration defined as the number of Li ions per unit volume (equal to  $x/\Omega$ ). It is useful to factor the chemical diffusion coefficient into a jump-diffusion coefficient,  $D_J$ , and a thermodynamic factor,  $\Theta$ , according to  $D = D_J\Theta$  where

$$D_J = \frac{kT}{x}\Omega\Lambda L \quad \text{and} \quad \Theta = \frac{\partial\left(\frac{\mu_{\text{Li}}}{kT}\right)}{\partial\ln x}$$

The volume factor,  $\Lambda$ , is equal to  $[1 - (\partial\ln\Omega/\partial\ln x)]^{-1}$  and accounts for the variation of the volume on Li concentration. Setting  $\Lambda$  equal to 1 is equivalent to neglecting the concentration dependence of the volume. The jump-diffusion coefficient is related to the mobility according to  $D_J = kT\Lambda M$ .

The thermodynamic factor,  $\Theta$ , measures the deviation of the intercalation compound from thermodynamic ideality, being equal to 1 for an ideal solution. It is a quantity that can easily be extracted from a measured voltage curve relative to a metallic Li reference anode. In Li intercalation compounds, the thermodynamic factor often deviates substantially from 1 at nondilute concentrations, diverging at Li compositions where Li-vacancy ordering is stable.<sup>10,24</sup>

The jump-diffusion coefficient,  $D_J$ , measures the ease with which Li ions collectively migrate within the intercalation compound crystal structure. While it is a kinetic coefficient, describing the response of the solid removed from equilibrium, it can nevertheless be related to fluctuations in Li density that occur at thermal equilibrium according to a Kubo-Green expression<sup>25,26</sup>

$$D_J = \frac{1}{2td} \left\langle \frac{1}{N} \left( \sum_{i=1}^N \Delta\vec{R}_i(t) \right)^2 \right\rangle$$

where  $d$  is the dimension of the interstitial network over which Li diffuses,  $N$  is the number of diffusing Li ions, and  $\Delta\vec{R}_i(t)$  is the vector that connects the trajectory of Li ion  $i$  after a time  $t$ . The angular brackets denote an ensemble average in the usual statistical mechanical sense and the

term within the brackets is related to the square of the displacement of the center of mass of the Li ions at equilibrium. The expression for each measure of Li mobility (i.e.,  $L$ ,  $M$ ,  $D$ , and  $D_j$ ) becomes a tensor for anisotropic crystal structures. The jump-diffusion coefficient can be calculated numerically using kinetic Monte Carlo simulations that sample representative Li trajectories.

### Diffusion in Thermodynamically and Kinetically Ideal Intercalation Compounds

Basic insight about the role of chemistry and crystal structure on Li mobility can be obtained by consideration of analytical expressions of  $D$  for thermodynamically and kinetically ideal intercalation compounds. We can extend the definition of a thermodynamically ideal intercalation compound to one that is also *kinetically ideal* by insisting that its migration barrier,  $\Delta E$ , for each Li hop is independent of the local degree of Li order/disorder. For these idealized intercalation compounds, the thermodynamic factor reduces to  $1/(1-x)$  while the jump-diffusion coefficient can be shown to be<sup>27</sup>

$$D_j = (1-x)\rho\lambda^2\Gamma$$

where  $\rho$  is a geometric factor that depends on the symmetry of the sublattice of interstitial sites and  $\lambda$  is the hop distance between adjacent interstitial sites. The hop frequency,  $\Gamma$ , can, as derived by Vineyard in the classical limit,<sup>28</sup> be approximated as

$$\Gamma = \nu^* \exp\left(-\frac{\Delta E}{kT}\right)$$

with  $\nu^*$  being a vibrational prefactor. (This expression is derived in the classical limit of the Harmonic approximation and more rigorous estimates within a quantum mechanical description can also be used as was done, for example, in ref 29. In this study, the difference between a classical and quantum mechanical treatment of hop frequencies is of the order of 30% at room temperature). While the jump-diffusion coefficient scales directly with vacancy concentration  $(1-x)$ , decreasing as the Li concentration of the host increases, the chemical diffusion coefficient, obtained by multiplying  $D_j$  with  $\Theta$  to yield

$$D = \rho\lambda^2\Gamma$$

has no explicit concentration dependence. Any variation of the chemical diffusion coefficient  $D$  with Li concentration in an ideal intercalation compound therefore

arises from a dependence of the activation barrier and vibrational prefactors on the average Li concentration. Due to the exponential dependence of  $D$  on  $\Delta E$ , a small variation in the migration barrier due to compositional, chemical or crystallographic changes translates into a large change in the diffusion coefficient, especially at room temperature.

The role of the dimensionality and connectivity of the interstitial network on  $D$  manifests itself in the geometric factor,  $\rho$ , which for interstitial sites that form a lattice is equal to  $z/2d$  with  $z$  the coordination number and  $d$  the dimension of the lattice. The geometric factor is equal to 1 for a cubic (three-dimensional), square (two-dimensional), and linear (one-dimensional) interstitial network, showing that there is no particular advantage gained by using intercalation compounds with three-dimensional interstitial networks. Larger geometric factors occur in crystal structures with high coordination numbers  $z$ .

### Diffusion in Nonideal Intercalation Compounds

The above expressions for Li diffusion coefficients are usually inadequate in describing transport in real intercalation compounds, except when the Li concentration is very dilute or very concentrated.<sup>30</sup> Additional complexities arise at intermediate Li concentrations where varying degrees of short and long-range order among Li ions are possible. Furthermore, unique crystallographic features of intercalation compounds lead to complex migration mechanisms that can result in a strong concentration dependence of the Li diffusion coefficient. In this context, it is both the nature of the anion sublattice and the arrangement of cations over the interstitial sites that in large part determine the mechanism of Li hops as well as their migration barriers. We illustrate this with  $\text{Li}_x\text{TiS}_2$ , one of the first intercalation compounds used in Li batteries<sup>16</sup> that has many crystallographic features in common with important oxide intercalation compounds.  $\text{Li}_x\text{TiS}_2$  can be synthesized as having either a layered or a spinel crystal structure with Li occupying the octahedral sites in both structures. Both forms of  $\text{Li}_x\text{TiS}_2$  exhibit a solid solution with respect to Li-vacancy disorder at room temperature allowing us to isolate the role of host crystal structure on Li diffusion from other complicating factors, such as phase transformations, order-disorder reactions and more complex electronic effects involving charge localization.

Energetically, the least hindered hop path between neighboring octahedral sites of a close-packed anion

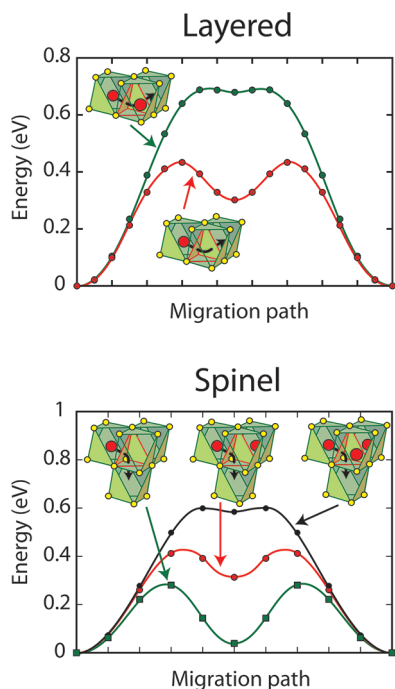


**FIGURE 4.** Li migration barriers for hops between neighboring octahedral sites in layered and spinel  $\text{LiTiS}_2$  are very sensitive to the occupancy of sites adjacent to the intermediate tetrahedral site of the hop. The barrier for hops into isolated vacancies is significantly larger than for divacancy hops and triple vacancy hops.

sublattice is along a curved path that passes through an adjacent tetrahedral site (Figure 2).<sup>10,11,14</sup> The energy of an intermediate tetrahedral site depends on the extent with which it is coordinated by neighboring cations. In the layered host, for example, a Li ion passing through a particular tetrahedral site could hop into a single vacancy or into a divacancy as illustrated in Figure 2c. Migrating into a single vacancy results in strong Li–Li interactions since the intermediate tetrahedral site shares a face with an occupied octahedral site. When hopping into a divacancy, however, this repulsion is absent and the migration barrier becomes significantly smaller than that for hops into isolated vacancies. First-principles calculations of the energy along the migration path confirm this as illustrated in Figure 4a. As is clear from Figure 4a, the tetrahedral site is a local minimum and can be quite stable for a divacancy hop. The same behavior is predicted for Li hops between adjacent octahedral sites in the spinel form of  $\text{Li}_x\text{TiS}_2$ . Due to the three-dimensional nature of this host structure, however, the intermediate tetrahedral sites are 4-fold coordinated by octahedral Li-sites. Li can now not only hop into isolated vacancies and divacancies, but also into triple vacancies. Following the same trend as in the layered compound, the migration barriers and the energies of the intermediate

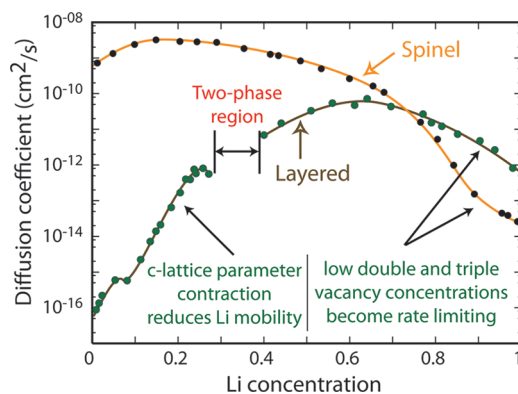


**FIGURE 5.** The variation of the chemical diffusion coefficients with Li concentration for layered and spinel  $\text{Li}_x\text{TiS}_2$  is substantially different, showing the importance of crystal structure on Li diffusion coefficients. Layered intercalation compounds usually undergo a contraction along the *c*-axis as the Li concentration is reduced, resulting in higher migration barriers and a reduction of the diffusion coefficient as *x* decreases. Li diffusion in spinel is primarily mediated by triple vacancies and divacancies, while divacancies mediate Li transport in layered  $\text{Li}_x\text{TiS}_2$ . Vacancy cluster diffusion mechanisms result in a strong concentration dependence of the diffusion coefficient at high Li concentrations where the vacancy concentration is low.

tetrahedral sites decrease as the number of vacancies surrounding the intermediate tetrahedral site increases as illustrated in Figure 4b.

As the  $\text{LiTiS}_2$  example illustrates, the structural constraints imposed by the close-packed stacking of the anion sublattice and the particular transition metal ion ordering over a subset of the interstitial sites lead to Li hop mechanisms that favor vacancy clusters: divacancies in the two-dimensional layered intercalation compounds and triple vacancies in three-dimensional compounds. The fact that the migration barriers for Li hops into vacancy clusters are significantly lower than into isolated vacancies means that diffusion is predominantly mediated by vacancy clusters. This was confirmed by kinetic Monte Carlo simulations.<sup>10,11,14</sup> Divacancy and triple-vacancy diffusion mechanisms lead to strong concentration dependencies of the chemical diffusion coefficient *D*, even in thermodynamically ideal intercalation compounds. Neglecting any deviation from thermodynamic ideality, the thermodynamic factor,  $\Theta$ , scales with the inverse of the vacancy concentration. Meanwhile, the jump-diffusion coefficient scales with the concentration of diffusion mediating defects, which for divacancies is to first order (neglecting short-range order among vacancies) proportional to the vacancy concentration squared and for triple vacancies proportional to the vacancy concentration cubed. Hence, any diffusion mediated by a vacancy cluster will have an explicit vacancy concentration dependence, which

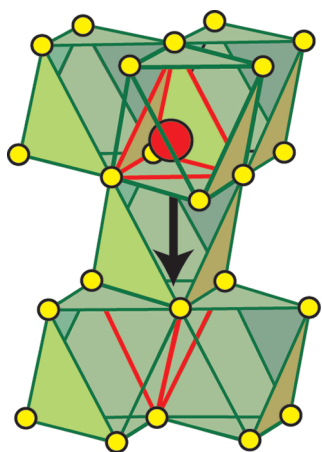


**FIGURE 6.** Li migration between neighboring tetrahedral sites of spinel oxides,  $\text{Li}_x\text{M}_2\text{O}_4$ , with  $x < 1$  pass through intermediate octahedral sites. Only the initial and final tetrahedral sites of a hop coordinate the intermediate octahedral site, and are empty when Li passes through the activated state, rendering a vacancy cluster diffusion mechanism impossible in these compounds.

decreases as the Li concentration increases. Kinetic Monte Carlo simulations of Li diffusion in layered and spinel  $\text{Li}_x\text{TiS}_2$ <sup>11,14</sup> predict this qualitative trend at high Li concentrations ( $x > 0.5$ ) as illustrated in Figure 5, showing that the decrease in diffusion coefficient in the three-dimensional spinel structure is more pronounced than in the two-dimensional layered structure.

Variations of the lattice parameter in layered intercalation compounds have also been shown to cause a strong concentration dependence of the diffusion coefficient.<sup>10,11</sup> Contraction of the *c*-lattice parameter of layered intercalation compounds as Li is removed leads to dramatic increases in the Li migration barriers. This results in a reduction of the Li diffusion coefficient as Li is removed, particularly below  $x = 0.5$  in  $\text{Li}_x\text{MO}_2$  or  $\text{Li}_x\text{TiS}_2$ .

Diffusion in intercalation compounds is not always mediated by vacancy clusters, even if they have a close-packed anion sublattice. Li ions in spinel oxides such as  $\text{Li}_x\text{Mn}_2\text{O}_4$  and  $\text{Li}_x\text{Ti}_2\text{O}_4$  occupy tetrahedral sites when  $x < 1$ . Lithium hops between adjacent tetrahedral sites pass through intermediate octahedral sites, which are the activated state in  $\text{Li}_x\text{Ti}_2\text{O}_4$ .<sup>12</sup> The intermediate octahedral sites are only coordinated by two tetrahedral sites, one being the initial state of the hop and the other the final state of the hop (Figure 6). This low coordination of the intermediate activated state by Li sites renders a vacancy cluster mechanism for diffusion impossible and Li diffusion proceeds through a single vacancy mechanism at all Li concentrations.

Other factors, in addition to vacancy cluster diffusion mechanisms, can result in a strong concentration dependence

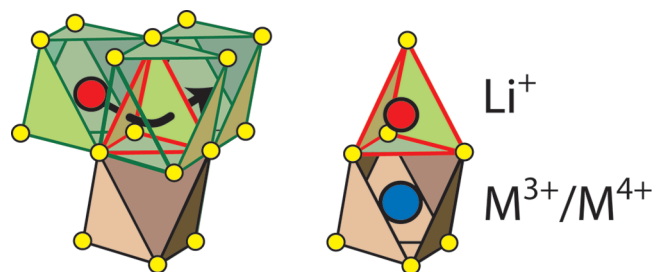


**FIGURE 7.** The intermediate tetrahedral site of Li hops in layered intercalation compounds having an ABC close-packed anion sublattice stacking shares a face with a transition metal ion. Removal of Li from  $\text{LiMO}_2$  results in a progressive increase in the effective valence of the transition metal ion resulting in larger electrostatic repulsions in the activated state that cause an increase in the migration barrier with decreasing Li concentration.

of the Li diffusion coefficient. In layered transition metal oxides such as  $\text{LiCoO}_2$ ,  $\text{Li}_x\text{NiO}_2$  and  $\text{Li}_x(\text{Co}_{1/3}\text{Ni}_{1/3}\text{Mn}_{1/3})\text{O}_2$ , where Li diffusion is mediated by divacancies, the intermediate tetrahedral site shares a face with an oxygen octahedron containing a transition metal as illustrated in Figure 7. Any change in the effective valence of the transition metal cation with Li concentration will affect the energy of Li occupancy in the tetrahedral site more than in the initial octahedral site. In general, this leads to an increase in the migration barrier as Li is removed since the effective valence of the transition metal increases from  $\text{M}^{3+}$  to  $\text{M}^{4+}$ .<sup>8,10</sup> Alloyed layered intercalation compounds such as  $\text{Li}_x(\text{Ni}_y\text{Co}_z\text{Mn}_{1-y-z})\text{O}_2$  have additional complexities due to relative differences in electron affinities between the various transition metal cations. For example, in  $\text{Li}_x(\text{Ni}_{0.5}\text{Mn}_{0.5})\text{O}_2$ , Ni cations tend to draw charge away from Mn, resulting in mixtures of  $\text{Ni}^{2+}$  and  $\text{Mn}^{4+}$  in the fully lithiated compound.<sup>31</sup> Hence, a Li hop that passes through tetrahedra sharing a face with a Ni octahedron will have a lower barrier than one passing in the vicinity of  $\text{Mn}^{4+}$ . Localized charge ordering and variations in oxidation states on transition metal ions in the spinel crystal structure can also introduce a concentration dependence on the Li migration barrier when migrating between tetrahedral sites.<sup>32</sup>

More subtle electronic effects can introduce a strong concentration dependence of the migration barriers for Li hops in intercalation compounds as well. Several transition metal oxides, for example, undergo Jahn–Teller distortions as their effective oxidation state is varied due to Li insertion or extraction. The resulting dimensional changes of the host crystal structure affect the activated state differently than the initial state and thereby also the migration barrier. The migration barrier for Li hops in anatase, for example, is very different depending on whether the Li concentration is dilute



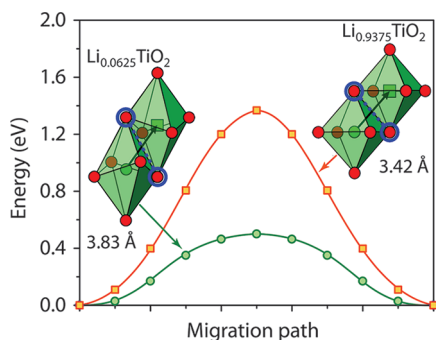


**FIGURE 8.** Li migration barriers in anatase  $\text{Li}_x\text{TiO}_2$  at dilute ( $x = 0.0625$ ) and concentrated ( $x = 0.9375$ ) Li concentrations. The migration barrier increases dramatically with Li concentration.

(i.e.,  $x \sim 0$ ) or whether it is very concentrated ( $x \sim 1$ ) due to the change in the degree of octahedral  $\text{TiO}_6$  distortions as Li is added to the host. In contrast to layered and spinel crystal structures, Li migration in the anatase crystal structure must pass through a pair of oxygen ions as illustrated in Figure 8. In the dilute limit, the oxygen octahedra around the Ti cations are highly distorted due to a second order Jahn–Teller effect around  $\text{Ti}^{4+}$  cations. This distortion opens up the Li migration path by increasing the distance of adjacent oxygen ions in the activated state. An increase in the overall Li concentration, however, leads to a progressive reduction of the Ti cations and causes a straightening out of the  $\text{TiO}_6$  octahedra, thereby constricting the activated state and resulting in a dramatic increase in the migration barrier. The concomitant large drop in the Li diffusion coefficient with increasing Li concentration is likely to be a factor that prevents full Li intercalation in anatase  $\text{TiO}_2$  in large particles.<sup>33</sup>

## Conclusion

The Li diffusion coefficient of an intercalation compound is a crucial kinetic parameter that determines how rapidly Li can be removed and reinserted into the compound. The Li diffusion coefficient and its concentration dependence is strongly affected by crystal structure and chemistry. Here we reviewed relevant equations describing Li mobility in intercalation compounds used as electrodes in Li-ion batteries. A crucial insight is that various crystallographic features common to many intercalation compounds will often introduce a strong concentration dependence of the Li diffusion coefficient. This is especially true if vacancy clusters mediate Li diffusion. For example, Li diffusion in layered intercalation compounds, including  $\text{Li}_x\text{CoO}_2$ ,  $\text{Li}_x\text{TiS}_2$ , and alloyed compounds  $\text{Li}_x(\text{Co}_y\text{Ni}_z\text{Mn}_{1-y-z})\text{O}_2$ , are mediated by divacancies. In intercalation compounds having a three-dimensional Li network, diffusion may even be mediated by triple

vacancies, as is predicted for spinel  $\text{Li}_x\text{TiS}_2$ . Diffusion mediated by vacancy clusters is likely to occur if three or more Li sites directly coordinate the intermediate activated state of Li hops. A concentration dependence of the diffusion coefficient also occurs in crystal structures susceptible to large lattice parameter variations with Li concentration, in crystal structures where the activated state is coordinated by transition metal cations, whose effective valence changes with Li concentration, and in compounds that undergo electronically induced distortions. These insights, generated in large part from comprehensive first-principles statistical mechanical studies of diffusion, will prove invaluable in the design of new electrode materials that are specifically optimized to have a particular concentration dependence of the Li diffusion coefficient.

*This material is based upon work supported as part of the Northwestern Center for Chemical Energy Storage, an Energy Frontier Research Center funded by the U.S. Department of Energy, Office of Science, Office of Basic Energy Sciences under Award Number DESC0001294. Computational resources provided by TERAGRID DMR100093 are also gratefully acknowledged.*

## BIOGRAPHICAL INFORMATION

**Anton Van der Ven** received a Ph.D. degree in Materials Science from MIT in 2000 and an engineering degree in Metallurgy and Applied Materials Science from the University of Louvain, Belgium in 1994. He joined the University of Michigan as an assistant professor in 2005, following a post doc at MIT. He is currently an associate professor in Materials Science and studies the thermodynamic, kinetic, and mechanical properties of materials for energy storage and structural applications.

**Jishnu Bhattacharya** is currently a postdoctoral researcher in the Materials Science Department at Northwestern University. He received his BE degree in Mechanical Engineering in 2002 from Bengal Engineering College, India, his MSc degree from Indian Institute of Science in 2005 and earned his PhD degree from University of Michigan in 2010. His research interests include the theoretical investigation of structural stability, solubility and diffusion in energy storage materials.

**Anna A. Belak** is a graduate student in Materials Science at the University of Michigan and received a Bachelors degree in Physics from Virginia Tech in 2008. Her research interests include the development and application of first-principles statistical mechanical tools in the study of materials for energy storage applications.

## FOOTNOTES

The authors declare no competing financial interest.

## REFERENCES

- Amatucci, G. G.; Tarascon, J. M.; Klein, L. C.  $\text{CoO}_2$ , the end member of the  $\text{Li}_x\text{CoO}_2$  solid solution. *J. Electrochem. Soc.* **1996**, *143* (3), 1114–1123.

- 2 Van der Ven, A.; Aydinol, M. K.; Ceder, G. First-principles evidence for stage ordering in  $\text{Li}_x\text{CoO}_2$ . *J. Electrochem. Soc.* **1998**, *145* (6), 2149–2155.
- 3 Chen, Z. H.; Lu, Z. H.; Dahn, J. R. Staging phase transitions in  $\text{Li}_x\text{CoO}_2$ . *J. Electrochem. Soc.* **2002**, *149*, A1604.
- 4 Wilkening, M.; Kuchler, W.; Heitjans, P. From ultraslow to fast lithium diffusion in the 2D ion conductor  $\text{Li}_{0.7}\text{TiS}_2$  probed directly by stimulated-echo NMR and nuclear magnetic relaxation. *Phys. Rev. Lett.* **2006**, *97* (6), 065901.
- 5 Grey, C. P.; Dupre, N. NMR Studies of Cathode Materials for Lithium-Ion Rechargeable Batteries. *Chem. Rev.* **2004**, *104*, 4493–4512.
- 6 Wagemaker, M.; Kentgens, A. P. M.; Mulder, F. M. Equilibrium lithium transport between nanocrystalline phases in intercalated  $\text{TiO}_2$  anatase. *Nature* **2002**, *418*, 397–399.
- 7 Verhoeven, V. W. J.; de Schepper, I. M.; Nachtegaal, G.; Kentgens, A. P. M.; Kelder, E. M.; Schoonman, J.; Mulder, F. M. Lithium dynamics in  $\text{LiMn}_2\text{O}_4$  probed directly by two-dimensional Li-7 NMR. *Phys. Rev. Lett.* **2001**, *86*, 4314–4317.
- 8 Van der Ven, A.; Ceder, G. Lithium diffusion in layered  $\text{Li}_x\text{CoO}_2$ . *Electrochem. Solid State Lett.* **2000**, *3* (7), 301–304.
- 9 Van der Ven, A.; Ceder, G. Lithium diffusion mechanisms in layered intercalation compounds. *J. Power Sources* **2001**, *97–8*, 529.
- 10 Van der Ven, A.; Ceder, G.; Asta, M.; Tepeš, P. D. First principles theory of ionic diffusion with non-dilute carriers. *Phys. Rev. B* **2001**, *64*, 184307.
- 11 Van der Ven, A.; Thomas, J. C.; Xu, Q.; Swoboda, B.; Morgan, D. Non-dilute diffusion in layered intercalation compounds:  $\text{Li}_x\text{TiS}_2$ . *Phys. Rev. B* **2008**, *78*, 104306.
- 12 Bhattacharya, J.; Van der Ven, A. Phase stability and non-dilute diffusion in lithium titanium spinel. *Phys. Rev. B* **2010**, *81*, 104304.
- 13 Persson, K.; Hinuma, Y.; Meng, Y. S.; Van der Ven, A.; Ceder, G. Thermodynamic and kinetic properties of the Li-graphite system from first principles calculations. *Phys. Rev. B* **2010**, *82* (12), 125416.
- 14 Bhattacharya, J.; Van der Ven, A. First-principles study of competing mechanisms of non-dilute Li diffusion in spinel  $\text{Li}_x\text{Ti}_2\text{S}_4$ . *Phys. Rev. B* **2011**, *83*, 144302.
- 15 Delmas, C.; Fouassier, C.; Hagenmuller, P. Structural classification and properties of the layered oxides. *Physica B+C* **1980**, *99* (1–4), 81–85.
- 16 Whittingham, M. S. Lithium batteries and cathode materials. *Chem. Rev.* **2004**, *104* (10), 4271–4301.
- 17 Van der Ven, A.; Aydinol, M. K.; Ceder, G.; Kresse, G.; Hafner, J. First-principles investigation of phase stability in  $\text{Li}_x\text{CoO}_2$ . *Phys. Rev. B* **1998**, *58* (6), 2975–22987.
- 18 Wolverton, C.; Zunger, A. First-principles prediction of vacancy order-disorder and intercalation battery voltages in  $\text{Li}_x\text{CoO}_2$ . *Phys. Rev. Lett.* **1998**, *81*, 606–609.
- 19 Zhou, F.; Maxisch, T.; Ceder, G. Configurational electronic entropy and the phase diagram of mixed-valence oxides: The case of  $\text{Li}_x\text{FePO}_4$ . *Phys. Rev. Lett.* **2006**, *97* (15), 155704.
- 20 Van der Ven, A.; Ceder, G. Ordering in  $\text{Li}_x(\text{Ni}_{0.5}\text{Mn}_{0.5})\text{O}_2$  and its relation to charge capacity and electrochemical behavior in rechargeable batteries. *Electrochem. Commun.* **2004**, *6* (10), 1045–1050.
- 21 Maxisch, T.; Zhou, F.; Ceder, G. Ab initio study of the migration of small polarons in olivine  $\text{Li}_x\text{FePO}_4$  and their association with lithium ions and vacancies. *Phys. Rev. B* **2006**, *73* (10), 104301.
- 22 Brian, E.; Laura, K. P.; Dominic, H. R.; Nazar, L. F. Small polaron hopping  $\text{Li}_x\text{FePO}_4$  solid solutions: Coupled lithium-ion and electron mobility. *J. Am. Chem. Soc.* **2006**, *128* (35), 11416–11422.
- 23 The emergence of internal electric fields due to insufficient screening by sluggish electrons then requires the introduction of electrochemical potentials and the Li flux becomes proportional not only to the gradient in the Li electrochemical potential but also the gradient of the electron electrochemical potential.
- 24 Jang, Y. I.; Neudecker, B. J.; Dudney, N. J. Lithium diffusion in  $\text{Li}_x\text{CoO}_2$  ( $0.45 < x < 0.7$ ) intercalation cathodes. *Electrochem. Solid State Lett.* **2001**, *4* (6), A74–A77.
- 25 Gomer, R. Diffusion of adsorbates on metal-surfaces. *Rep. Prog. Phys.* **1990**, *53* (7), 917–1002.
- 26 Zwanzig, R. Elementary derivation of time-correlation formulas for transport coefficients. *J. Chem. Phys.* **1964**, *40* (9), 2527.
- 27 Kutner, R. Chemical Diffusion in the lattice gas of non-interacting particles. *Phys. Lett.* **1981**, *81A*, 239.
- 28 Vineyard, G. H. Frequency factors and isotope effects in solid state rate processes. *J. Phys. Chem. Solids* **1957**, *3*, 121.
- 29 Toyoura, K.; Koyama, Y.; Kuwabara, A.; Oba, F.; Tanaka, I. First-principles approach to chemical diffusion of lithium atoms in a graphite intercalation compound. *Phys. Rev. B* **2008**, *78*, 214303.
- 30 Morgan, D.; Van der Ven, A.; Ceder, G. Li conductivity in  $\text{Li}_x\text{MPO}_4$  ( $M = \text{Mn, Fe, Co, Ni}$ ) olivine materials. *Electrochem. Solid State Lett.* **2004**, *7*, A30.
- 31 Kang, K.; Ceder, G. Factors that affect Li mobility in layered lithium transition metal oxides. *Phys. Rev. B* **2006**, *74*, 094105.
- 32 Bo, X.; Meng, S. Factors affecting Li mobility in spinel  $\text{LiMn}_2\text{O}_4$  — A first-principles study by GGA and GGA+U methods. *J. Power Sources* **2010**, *195* (15), 4971–4976.
- 33 Borghols, W. J. H.; Lutzenkirchen-Hecht, D.; Haake, U.; van Eck, E. R. H.; Mulder, F. M.; Wagemaker, M. The electronic structure and ionic diffusion of nanoscale  $\text{LiTiO}_2$  anatase. *Phys. Chem. Chem. Phys.* **2009**, *11*, 5742–5748.